Available online at www.sciencedirect.com
SCIENCE DIRECT®

Journal of the European Ceramic Society 24 (2004) 2575–2581
www.elsevier.com/locate/jeurceramsoc

A statistical approach to the identification of determinant factors in the preparation of phase pure $(Bi,La)_4Ti_3O_{12}$ from an aqueous citrate gel

An Hardy, Geert Vanhoyland, Marlies Van Bael, Jules Mullens*, Lucien Van Poucke

Laboratory of Inorganic and Physical Chemistry, Limburgs Universitair Centrum, B-3590 Diepenbeek, Belgium

Received 24 May 2003; received in revised form 19 September 2003; accepted 27 September 2003

Abstract

The factors influencing crystallization of layered-perovskite lanthanum substituted bismuth titanate, starting from an aqueous metal-chelate precursor-gel, were identified by means of statistically designed experiments. To ensure experimental economy and efficiency in spite of the large number of factors possibly affecting the phase purity, a fractional factorial design was chosen. The calcination atmosphere turned out to be the most important to avoid the formation of the Sillenite secondary phase, $Bi_{12}TiO_{20}$. In order to study its impact on phase purity thoroughly an extensive number of ambient compositions were tested. These tests showed that dry air is the optimal composition. Precursor stoichiometry and gas flow rate during heat treatment also significantly influenced the formation of $Bi_{12}TiO_{20}$. Furthermore, the precursor stoichiometry and cooling rate as well as the calcination atmosphere and crystallization time turned out to interact.

Keywords: Perovskites; Powders-chemical preparation; Sol-gel processes; Statistical design; X-ray methods; $(Bi,La)_4Ti_3O_{12}$

1. Introduction

Bismuth titanate ($Bi_4Ti_3O_{12}$, BiT) belongs to a family of layer-structured perovskites, which was first described by Aurivillius.[1] Its structure consists of $Bi_2O_2^{2+}$ layers interleaved with $Bi_2Ti_3O_{10}^{2-}$ perovskite layers, which are stacked along the *c*-axis. Based on XRD measurement its unit cell was found to be orthorhombic.[1] From optical and electrical measurements however, a monoclinic structure was suggested.[2] BiT has ferroelectric properties with a Curie temperature (T_C) of 675 °C and a high remanent polarization ($P_r = 50$ μC/cm^2 along the *a*-axis of the single crystal).[3] Due to these excellent properties it was considered to be a candidate material for the fabrication of thin film capacitors used as non-volatile RAMs. Unfortunately, it also suffers from fatigue, meaning that the remanent polarization decreases with increasing number of switching cycles. Recently Park et al. found that substituting a small amount of lanthanum for bismuth provides a solution for this drawback.[4]

BiT as well as BLT powders have been prepared in our laboratory by different aqueous solution-gel routes.[5–7] These chemical processes provide a high degree of homogeneity in the precursor phase, which is maintained during the thermal treatment,[5,6] and subsequently leads to a lower crystallization temperature of the desired Aurivillius phase. Synthesis of BLT by a traditional solid-state route requires temperatures of at least 900 °C and long firing times.[8] In our laboratory however, it was shown recently, by high-temperature XRD, that the thermo-oxidative decomposition of an aqueous metal-chelate gel led to the formation of phase pure BLT at temperatures as low as 525 °C, without the formation of an intermediate pyrochlore phase.[5]

Contrary to this good result, it turned out to be difficult to prepare the phase pure oxide in a conventional furnace with dynamic atmosphere due to the formation of a secondary phase, which was identified as $Bi_{12}TiO_{20}$ (JCPDS 34-0079) by XRD analysis. This phase has a body-centred cubic structure called Sillenite, the same as is associated to the γ-phase of Bi_2O_3.[9]

According to Narendar and Messing[10] the phase formation of multimetal oxides, by calcination of metal-carboxylate gel precursors, occurs through complicated

* Corresponding author. Tel.: +32-11-26-83-08; fax: +32-11-26-83-01.
E-mail address: jules.mullens@luc.ac.be (J. Mullens).

0955-2219/$ - see front matter © 2003 Elsevier Ltd. All rights reserved.
doi:10.1016/j.jeurceramsoc.2003.09.018

mechanisms which are affected by the heat release rate and heat dissipation rate throughout the sample bed, the availability of oxygen, chemical kinetics of the decomposition reactions, etc.

In order to study in a systematic yet economic way the effect of the many factors involved with BLT phase formation, in this work a fractional factorial design was applied following Box et al.[11] These designs allow identification of interactions between factors, leading to non-additive effects on the response. To our knowledge the DOE (design of experiments) approach has been applied only sporadically to multimetal oxide synthesis.[12,13]

In this paper, the optimization of the calcination and crystallization conditions for obtaining phase pure BLT is reported and an explanation for the observed phase separation is proposed.

2. Experimental

2.1. Precursor synthesis and calcinations

A BLT precursor solution is prepared by combination of aqueous solutions of bismuth citrate, lanthanum citrate and a peroxocitrato–Ti(IV) complex, as is described elsewhere.[5] A glassy and amorphous aqueous metal-chelate gel was synthesized by evaporation of this precursor solution in a furnace at 60 °C. The composition $Bi_{3.5}La_{0.5}Ti_3O_{12}$ was chosen due to its high P_r and consequent relevance in the production of thin film ferroelectric RAMs.

For each heat treatment (specified in Section 2.3.1), 50 mg of the precursor was used. They were carried out in a TGA furnace (TA Instruments TGA 951-2000) using quartz sample pans. The furnace was flushed before the start of the heating schedule in order to assure the presence of the correct calcination atmosphere (synthetic air or oxygen).

2.2. Powder characterization and definition of a quality indicator

The multimetal oxide final product was characterized by means of powder X-ray diffraction. A Siemens D-5000 diffractometer (Cu-$K\alpha$ radiation) was used to take spectra from 10 to 35°2θ. The sample was sieved as a thin layer onto a Si(100) sample holder covered with silicone grease, in order to eliminate errors due to orientation of the powder and to assure a good adhesion during the θ–2θ goniometer movement. Additionally, the specimen was spinned to improve the counting statistics.

XRD is one of the most appropriate characterization techniques to distinguish the chemical identity of various crystalline phases in a mixture and to determine their precise amount. In the literature, several methods are described to carry out a quantitative analysis, e.g. by means of the Rietveld method, the RIR method, etc.[14] However, to draw conclusions from a statistical design it suffices to make a relative estimation of the phase purity to compare the different treatments and derive any trends.

The method used here is based on the relation between the integrated peak intensity in the XRD pattern and the amount of crystalline phase present in a mixture. This is linear only in a limited interval due to the occurrence of X-ray absorption effects, e.g. a difference in the linear absorption coefficient for phases that differ strongly qua composition, such as the Sillenite and layered perovskite phase. In order to check the linearity for these mixtures, a calibration curve was set up by mixing commercial BiT and $Bi_{12}TiO_{20}$ powders (Alfa Aesar, 99.9% metals basis). BLT was replaced by BiT since, to our knowledge, it is not commercially available itself. BiT has the same crystal symmetry as BLT for small amounts of La^{3+} substituted[15] and a not too different absorption coefficient (mass absorption coefficient μ/ρ equals 198.65 and 203.54 cm^2g^{-1} for $x=0.5$, respectively). Instead of directly relating the integrated intensity of a certain $Bi_{12}TiO_{20}$ peak to the intensities obtained from the calibration samples, the ratio was made with a specific Bragg peak of the $Bi_4Ti_3O_{12}$ main phase. In this way eventual instrumental effects, due to measuring of the different samples over a certain period of time, were compensated. The (310) Sillenite peak at 27.7°2θ and (111) Aurivillius peak at 23.3°2θ were selected. They do not overlap with other peaks and are positioned in each other's vicinity in the diffraction pattern, which avoids errors due to differences in diffraction volume.

The Alfa Aesar materials contained minor impurities as was shown by XRD: in case of BiT (JCPDS 35-0795) a small fraction of $Bi_{12}TiO_{20}$ was found, whereas the $Bi_{12}TiO_{20}$ contains some additional γ-Bi_2O_3 (JCPDS 45-1344). However, the presence of γ-Bi_2O_3 in the Sillenite, interfering with the (310) Sillenite peak, and the presence of Sillenite in the BiT will not alter the shape of the calibration plot, so it will still be possible to determine the interval of linearity.

The calibration graph (Fig. 1) shows the ratio A(310)/A(111) as a function of the weight percentage of unpurified Sillenite in BiT. A is the integrated peak intensity calculated by fitting a pseudo-Voigt function.

From this plot it is concluded that the detection limit of the Sillenite in BiT is below 1.5%. Moreover, it is clear that a linear response is obtained from 0 to 30% of secondary phase. Since all the powders prepared in the fractional factorial designs (see Section 2.3.1) were situated in this region, the quality indicator used in the following sections could be defined by Eq. (1). It is proportional to the amount of Sillenite phase. In the ideal case of a phase pure sample, it will be equal to 0.

$$Q.I. = \mathrm{A}(310)/\mathrm{A}(111) \quad (1)$$

After optimization of the heat treatment based on the experiments presented in the following paragraphs, it became possible to synthesize phase pure BLT powder. Commercial Sillenite was mixed with this powder, in order to check the assumption of similar behaviour for BLT and BiT. The results are presented in Fig. 1 as the dotted line, from which it is concluded again that linearity is assured up to 30% Sillenite.

2.3. Identification of factors determining phase purity

Based on preliminary experiments and literature, several factors concerning the precursor, calcination and crystallization conditions were suspected to affect the phase purity of the oxide obtained after gel thermolysis. Evidently, the Bi^{3+}-content of the precursorgel was thought to have a great influence. It was varied between 0 and 10 mol% excess. Recently it was found that this has an influence on the crystallization temperature of BLT as well.[5] The heating rate (5 or 20 °C/min), O_2 partial pressure (20 or 100%) and gas flow rate (15 or 50 ml/min) could affect the decomposition pathway and reaction kinetics of gel thermolysis. The crystallization atmosphere (N_2 or O_2), temperature (550 or 750 °C) and time (20 or 90 min) were expected to influence the transformation of possible intermediate secondary phases to the desired Aurivillius phase. Finally, the cooling rate was taken into account as well. These factors and their levels are summarized in Table 1. Note that the switch from calcination atmosphere to crystallization atmosphere, if necessary, was made as soon as the weight remained stable.

2.3.1. Singling out the most important factors and interactions

Fractional factorial designs allow screening of a large number of factors and singling out the most important ones.[11] A resolution IV fractional factorial design, requiring only 16 runs, was chosen here to estimate the main effects of the eight factors, free from two-factor interactions, and of seven sets of four confounded two-factor interactions. The settings of these sixteen runs are summarized in the design matrix of Table 2.[16] The first column shows the standard run order. In order to avoid any influence of uncontrollable variables such as time-effects, the actual run order was randomized as shown in the second column. During an experimental run the factors are set to the levels associated with the signs in the respective factor columns. The two-factor interactions columns will be used for data analysis. All three-factor and higher order interactions are considered negligible.

Some representative XRD spectra are shown in Fig. 2 for a well crystallized, but not phase pure sample (run 8 in the standard run order) as well as for a sample with smaller crystallite size and therefore broader peaks (run 2), for which no secondary phase was detected. Whenever the amount of secondary phase was below the detection limit of the XRD apparatus, the *Q.I.* was set equal to 0.

The quality indicators were calculated from these spectra and are summarized in the final column of Table 2.

2.3.1.1. Effects calculation—estimation of the impact of the factors and interactions on phase purity. The effect of a factor is defined as the change in response when its level changes from high to low as is formulated in Eq. (2).[11]

$$\text{Estimated} \quad \text{effect} = \mathrm{I} = \left(\Sigma(Q.I.)_{+} - \Sigma(Q.I.)_{-}\right)/8 \qquad (2)$$

These effects are summarized at the bottom of Table 2. A graphical representation is given in the estimated effects plot (Fig. 3),[16] where $\Sigma(Q.I.)_{+}/8$ and $\Sigma(Q.I.)_{-}/8$ are plotted for each factor or group of interactions.

From the estimated effects plot it is clear that the largest differences in *Q.I.* occur when changing factors 3, 1 and 4 as well as the group of four confounded

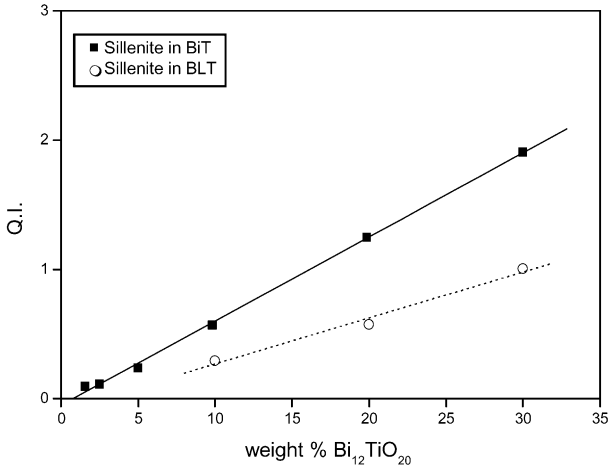

Fig. 1. Calibration graph: *Q.I.* as a function of the% (wt.) of $Bi_{12}TiO_{20}$ in commercial BiT (■) and in BLT (○).

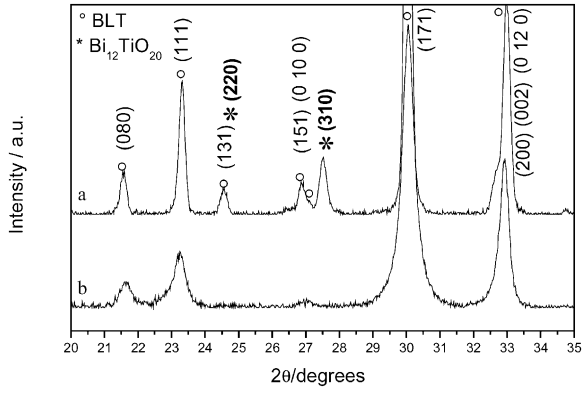

Fig. 2. XRD spectra for samples of (a) run 8 and (b) run 2.

Table 1
Factors and levels

	Factor	Low level (−)	High level (+)
1	Stoichiometry	Stoichiometric	10% Bi-excess
2	Heating rate	5 °C/min	20 °C/min
3	Calcination atmosphere	Synthetic dry air (80% N_2, 20% O_2)	Oxygen
4	Gas flow rate	15 ml/min	50 ml/min
5	Crystallization temperature	550 °C	750 °C
6	Crystallization time	20 min	90 min
7	Crystallization atmosphere	Nitrogen	Oxygen
8	Cooling rate	Slow in furnace	Quench to room temperature

Table 2
Resolution IV fractional factorial design matrix, calculated quality indicators and estimated effects

Standard order	Random order	Factors and groups of confounded interactions															*Q.I.*
		1	2	3	4	12 35 46 78	13 25 47 68	14 26 37 58	15 23 48 67	16 24 38 57	17 28 34 56	5	6	7	8	18 27 36 45	
1	3	−	−	−	−	+	+	+	+	+	+	−	−	−	−	+	0.00
2	8	−	−	−	+	+	+	−	+	−	−	−	+	+	+	−	0.00
3	16	−	−	+	−	+	−	+	−	+	−	+	−	+	+	−	0.33
4	2	−	−	+	+	+	−	−	−	−	+	+	+	−	−	+	0.37
5	14	−	+	−	−	−	+	+	−	−	+	+	+	−	+	−	0.00
6	9	−	+	−	+	−	+	−	−	+	−	+	−	+	−	+	0.00
7	12	−	+	+	−	−	−	+	+	−	−	−	+	+	−	+	0.20
8	1	−	+	+	+	−	−	−	+	+	+	−	−	−	+	−	0.52
9	4	+	−	−	−	−	−	−	+	+	+	+	+	+	−	−	0.094
10	5	+	−	−	+	−	−	+	+	−	−	+	−	−	+	+	0.047
11	7	+	−	+	−	−	+	−	−	+	−	−	+	−	+	+	0.48
12	10	+	−	+	+	−	+	+	−	−	+	−	−	+	−	−	0.63
13	13	+	+	−	−	+	−	−	−	−	+	−	−	+	+	+	0.00
14	6	+	+	−	+	+	−	+	−	+	−	−	+	−	−	−	0.17
15	11	+	+	+	−	+	+	−	+	−	−	+	−	−	−	−	0.47
16	15	+	+	+	+	+	+	+	+	+	+	+	+	+	+	+	0.44
ΣQ.I.$_-$/8		0.18	0.24	0.038	0.20	0.25	0.22	0.24	0.25	0.21	0.21	0.25	0.25	0.26	0.24	0.28	0.23
ΣQ.I.$_+$/8		0.29	0.22	0.43	0.27	0.22	0.25	0.23	0.22	0.25	0.26	0.22	0.22	0.21	0.23	0.19	Average
Estimated effect		0.11	−0.021	0.39	0.074	−0.025	0.036	−0.015	−0.027	0.040	0.045	−0.031	−0.031	−0.044	−0.013	−0.084	Q.I.

Twelve designates the interaction between factors 1 and 2, etc.

interactions 18, 27, 36 and 45 from their respective low to high levels. It is also easily seen from this plot that the best setting in order to minimize the *Q.I.* for the eight factors x_i is (x_1, x_2, x_3, x_4, x_5, x_6, x_7, x_8) = (−, +, −, −, +, +, +, +). This means that a stoichiometric BLT gel has to be heated at 20 °C/min in 15 ml/min dry air up to 750 °C, with a 90-min isothermal period in oxygen ambient, followed by quenching to room temperature. Three replicates of this heat treatment were applied to different batches of the gel to confirm this result. In all these experiments *Q.I.* = 0 was found, demonstrating the reproducible formation of phase pure BLT by means of these settings.

2.3.1.2. Deciding which of the impacts are significant. In order to determine which of the effects and accessory factors are significant, a normal plot was constructed (not shown).[11] It was concluded that the factors 1 (stoichiometry), 3 (calcination atmosphere) and 4 (gas flow rate) as well as the set of interactions 18, 27, 36, 45 are indeed the only ones distinguishable from noise.

This can be expressed by the factorial representation [Eq. (3)],[11] where each response is assumed to be the result of additional effects of the important factors and interactions. Here x_i (i = 1, 3, 4, 18) takes the value −1 or +1 according to the columns of signs in Table 3. Note that $x_{18} = x_{27} = x_{36} = x_{45}$.

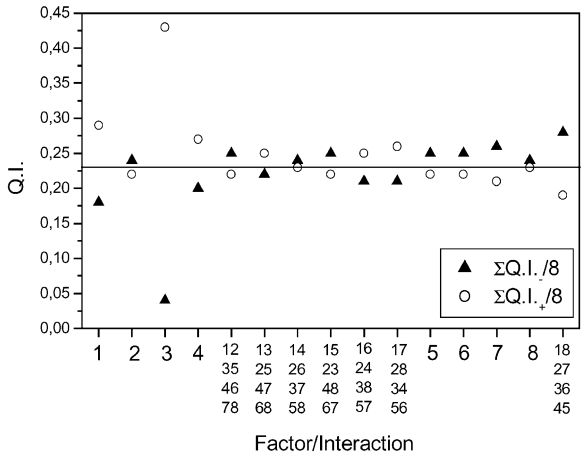

Fig. 3. Main effects and interaction effects plot.

Table 3
Augmenting design matrix and calculated Q.I

Standard order	Random order	Factors								*Q.I.*
		1	2	3	4	5	6	7	8	
17	2	−	−	+	+	+	−	+	−	0.38
18	1	−	+	−	+	−	+	+	−	0.00
19	4	+	−	−	+	−	−	+	+	0.00
20	3	+	+	+	+	+	+	+	+	0.31

$$\hat{Q}.I. = 0.23 + (0.11/2)x_1 + (0.39/2)x_3 + (0.074/2)x_4 + (-0.084/2)x_{18} \quad (3)$$

2.3.1.3. Double-checking validity of conclusions concerning significance. In order to check the accuracy of this model a normal plot of residuals,[17] calculated according to Eq. (4), was constructed (not shown).[11]

$$\text{Residual} = Q.I. - \hat{Q}.I. \quad (4)$$

The points of the residual normal plot were all close to the line, confirming that the deviations from the model were due to random variation only.

Experiments in which phase pure BLT was formed out of a stoichiometric BLT gel, heated in 15 ml/min of dry air while setting the five other factors to arbitrary levels for obtaining a high process efficiency (heating rate 20 °C/min, crystallization 55 min at 625 °C in oxygen, slow cooling to room temperature) supported the conclusions concerning factor significance.

2.3.2. De-aliasing of confounded interactions—gaining insight into the process properties

It was shown by the fractional factorial design that the effect of the set of confounded two-factor interactions 18, 27, 36, 45, all calculated together, was significant. In order to be able to estimate the effects of these four interactions separately, leading to a more profound insight into the process, four additional experiments have been carried out.[11]

The conditions during these tests were in accordance with the four-run design matrix shown in Table 3. The factors and their levels were the same as for the fractional factorial design (Table 1). The quality indicators calculated from the XRD spectra are shown in the last column of Table 3.

The data from the new design are combined with those from the former design according to the method described by Box et al.[11] The following individual values for the estimated interaction effects were calculated: $l_{18} = 0.14$, $l_{27} = -0.034$, $l_{36} = -0.15$ and $l_{45} = -0.043$. The interactions 18 and 36 are significant.

3. Discussion

Amorphous metal-chelate gel precursors are generally assumed to allow crystallization of the phase pure multimetal oxides at a lower temperature compared to conventional solid-state methods, due to the mixing of metalions at a molecular scale. This advantage is lost if phase separation occurs at the stage of gel formation due to precipitation of, e.g. hydrolyzed metalions or insoluble metal carboxylates. However, the aqueous citrate gel used as a precursor in this work has been shown to be amorphous and homogeneous down to a scale of at least ~10 nm by TEM.[5] Nonetheless, phase separation can also occur during gel thermolysis, for instance if the monometal complexes have different decomposition temperatures.[18] This leads to an inhomogeneous cation distribution directly prior to oxide crystallization, affecting the energy barriers to nucleation and growth of the oxide phase(s) from the amorphous precursor. Phase separation at the thermolysis stage is therefore a plausible explanation for the observations in this work.

3.1. The effect of precursor stoichiometry

Using a precursor containing 5% excess of Bi^{3+} has a negative influence on phase purity of the oxide, which is self-evident. It is clear that bismuth oxide volatilization does not occur at the chosen crystallization temperatures and times, so that the excess of bismuth remains in the oxide. In run 13 however, a precursor containing an excess of Bi^{3+} was used, but a *Q.I.* of 0 was calculated from the XRD. Nonetheless, an SEM study did show the presence of a bismuth rich secondary phase. This apparent contradiction is ascribed to the short crystallization time at low temperature and the high cooling rate, which in this particular case leads to

incompletely developed crystalline and/or amorphous phases. It is evident that the latter are not detected by XRD.

3.2. The effect of the calcination atmosphere

The influence of the oxygen partial pressure (pO_2) during gel decomposition is even larger than the effect of precursor stoichiometry. Using pure oxygen during gel thermolysis inevitably leads to the formation of the secondary phase. Using dry air however, enables the formation of phase pure BLT in some cases.

In order to study its impact on phase purity thoroughly, an increased number of ambient compositions were tested. The selected levels were 100, 75, 50, 20, 10 and 5% oxygen in nitrogen. Pure nitrogen was not used, since the organic fraction of the gel does not decompose completely at reasonably low temperatures in an inert atmosphere. The gas flow was always 15 ml/min except for the run in 5% O_2 where it was 20 ml/min due to technical limitations. A stoichiometric precursor gel was heated at 20 °C/min, followed by crystallization for 55 min at 625 °C in oxygen. From the XRD spectra the quality indicators were calculated. Only in 20% O_2, the composition of dry air, phase pure BLT was formed. With higher as well as with lower oxygen concentrations the secondary phase is formed. Its amount increases monotonically with $\%_{vol}(O_2)$ above 20%. The results are summarized in Fig. 4, showing the quality indicator as a function of the volume percentage of oxygen in the calcination atmosphere. It is clear that there is an optimum for the pO_2.

The observed effect is probably related to a change in decomposition pathway with a change in calcination atmosphere. An increase of the gel decomposition rate with increasing pO_2 was observed.

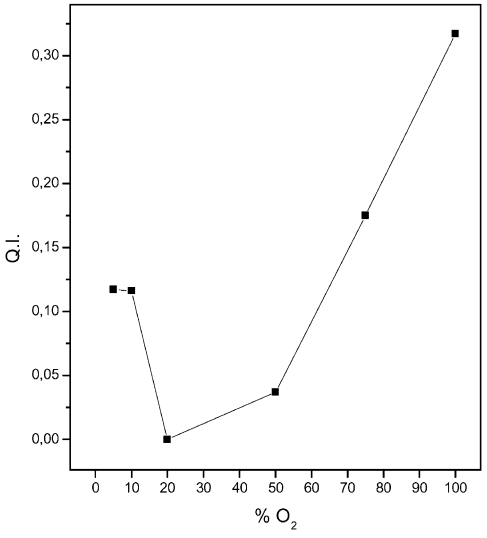

Fig. 4. Q.I. as a function of O_2 $\%_{(vol)}$ during calcinations.

3.3. The effect of gas flow rate

The gas flow rate had the smallest important effect on phase purity. The highest gas flow rate increased the amount of secondary phase compared with the lowest gas flow rate. Its effect is probably connected to the effect of oxygen partial pressure during calcination, since both a higher gas flow rate and a higher pO_2 lead to an increase in O_2 availability. In contrast with the pO_2, the gas flow rate turned out not to be systematically related to the gel decomposition rate. This indicates that an increase of the gel decomposition rate is not the only reason for phase separation.

3.4. Interactions

The interactions 18 and 36 were found to be significant. They can be interpreted by means of two-way tables (Fig. 5), constructed with data from the original 16 runs.[11] At the corners of the squares the average responses of the runs with the specified settings of the interacting factors are shown.

At a low cooling rate (factor 8) the sensitivity of phase purity towards a change in Bi^{3+} stoichiometry (factor 1) is much larger than at quenching. This may be explained by the formation of poorly crystalline or amorphous Bi^{3+}-rich secondary phases, when quenching the oxide(s) to room temperature.

When setting a short crystallization time (factor 6) the sensitivity towards a change in calcination atmosphere (factor 3) is larger than when a long crystallization time is applied. This is understandable since a longer crystallization time will allow more of the bismuth-rich secondary phase to transform into the Aurivillius phase by solid-state reaction with a titanium-rich phase. Such a phase must be present in all of the stoichiometric samples, even though it does not appear clearly in the XRD pattern. Indeed the presence of rutile TiO_2 (JCPDS 21-1276, 100% peak at 27.44°2θ) was shown by TEM selected area electron diffraction measurements for the product of run 3. The fact that this phase was not detected with XRD is probably due to the difference in

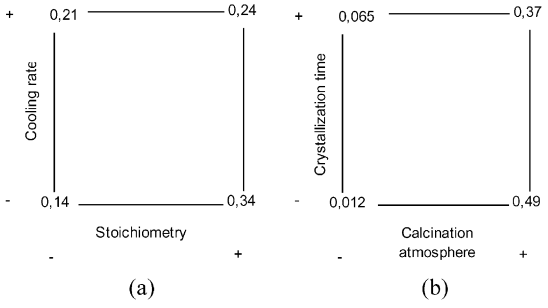

Fig. 5. Two-way tables of interacting factors (a) cooling rate and stoichiometry, (b) crystallization time and calcination atmosphere.

contrast between the TiO_2 and Sillenite, the small TiO_2 particle size (<100 nm), its low concentration and partial peak overlap with the Sillenite peak at 27.7°2θ. An estimation of the quantity of this phase would therefore have been very difficult, which is why the Sillenite phase is a better criterion for phase purity. Moreover, it is sufficient to calculate only the relative amount of $Bi_{12}TiO_{20}$, because if there is no phase separation of Bi^{3+}, a Ti^{4+}-rich phase will not be formed either.

4. Conclusion

A fractional factorial design has been applied successfully to obtain crystalline, phase pure lanthanum substituted bismuth titanate with the Aurivillius structure starting from an aqueous metal-chelate gel. It has been found that the calcination atmosphere, precursor stoichiometry and gas flow rate as well as one set of interactions are the determinant factors of phase purity of the final multimetal oxide. By augmenting the first fractional factorial design, it was found that interactions exist between the cooling rate and the stoichiometry as well as between the calcination atmosphere and the crystallization time, implying that the total effect of these factors is not a simple addition of their separate effects.

A study of the influence of oxygen partial pressure during calcination on phase purity, led to the conclusion that dry air is the optimal calcination ambient for the preparation of phase pure BLT.

A fast yet effective process to prepare Aurivillius phase BLT from the aqueous metal-chelate gel, is to heat the stoichiometric precursor in dynamic dry air (15 ml/min). The process speed is set relatively high by using a heating rate of 20 °C/min and an isothermal period of 55 min at 625 °C, which also leads to a well-crystallized product.

Due to the sensitivity of the final phase composition to the calcination atmosphere and gas flow rate, a further optimization was needed when the process was scaled up in a tube furnace (using 1.5 g of precursor gel). Here, the addition of a grinding step before completion of the precusor decomposition was necessary in order to avoid phase separation of $Bi_{12}TiO_{20}$.

Acknowledgements

A. Hardy is a research assistant and M.K. Van Bael and G. Vanhoyland are post-doctoral research fellows of the Fund for Scientific Research—Flanders, Belgium (FWO-Vlaanderen).

References

1. Aurivillius, B., Mixed bismuth oxides with layer lattices II. Structure of $Bi_4Ti_3O_{12}$. *Ark. Kemi*, 1949, **1**, 499–512.
2. Cummins, S. E. and Cross, L. E., Crystal symmetry, optical properties and ferroelectric polarization of $Bi_4Ti_3O_{12}$ single crystals. *Appl. Phys. Lett*., 1967, **10**, 14–15.
3. Cummins, S. E. and Cross, L. E., Electrical and optical properties of ferroelectric $Bi_4Ti_3O_{12}$ single crystals. *J. Appl. Phys*., 1968, **39**, 2268–2274.
4. Park, B. H., Kang, B. S., Bu, S. D., Noh, T. W., Lee, J. and Jo, W., Lanthanum-substituted bismuth titanate for use in non-volatile memories. *Nature*, 1999, **401**, 682–684.
5. Hardy, A., Mondelaers, D., Van Bael, M. K., Mullens, J., Van Poucke, L. C., Vahoyland, G. and D'Haen, J. Synthesis of $(Bi,La)_4Ti_3O_{12}$ by a new aqueous solution-gel method. *J. Eur. Ceram. Soc*., (in press).
6. Hardy, A., Mondelaers, D., Vanhoyland, G., Van Bael, M. K., Mullens, J. and Van Poucke, L. C., The formation of ferroelectric bismuth titanate ($Bi_4Ti_3O_{12}$) from an aqueous metal-chelate gel. *J. Sol-Gel Sci. Techn*., 2003, **26**, 1103–1107.
7. Hardy, A., Van Werde, K., Vanhoyland, G., Van Bael, M. K., Mullens, J. and Van Poucke, L. C., Study of the decomposition of an aqueous metal-chelate gel precursor for $(Bi,La)_4Ti_3O_{12}$ by means of TGA-FTIR, TGA-MS and HT-DRIFT. *Thermochim. Acta*, 2003, **397**, 143–153.
8. Noguchi, Y., Miwa, I., Goshima, Y. and Miyayama, M., Defect control for large remanent polarization in bismuth titanate ferroelectrics- Doping effect of higher-valent cations. *Jpn. J. Appl. Phys*., 2000, **39**, L1259–L1262.
9. Efendiev, S. M., Kulieva, T. Z., Lomonov, V. A., Chiragov, M. I., Grandolfo, M. and Vecchia, P., Crystal structure of bismuth titanium oxide $Bi_{12}TiO_{20}$. *Phys. Status Solidi A*, 1981, **74**, K17–K21.
10. Narendar, Y. and Messing, G. L., Kinetic analysis of combustion synthesis of lead magnesium niobate from metal carboxylate gels. *J. Am. Ceram. Soc*., 1997, **80**, 915–924.
11. Box, G. E. P., Hunter, W. G. and Hunter, J. S., *Statistics for Experimenters, An Introduction to Design, Data Analysis, and Model Building*. John Wiley and Sons, New York, 1978.
12. Viviani, M., Lemaitre, J., Buscaglia, M. T. and Nanni, P., Low-temperature aqueous synthesis (LTAS) of $BaTiO_3$: a statistical design of experiment approach. *J. Eur. Ceram. Soc*., 2000, **20**, 315–320.
13. Van Driessche, I., Persyn, F., Fiermans, L. and Hoste, S., A statistical Plackett-Burman design of the thermal process in the synthesis of the Bi-2223 HTSC. *Supercond. Sci. Tech*., 1996, **9**, 843–848.
14. Klug, H. P. and Alexander, L. E., *X-ray Diffraction Procedures: For Polycrystalline and Amorphous Materials*. John Wiley and Sons, New York, 1974.
15. Wolfe, R. W. and Newnham, R. E., Rare Earth Bismuth titanates. *J. Electrochem. Soc.: Sol. State Sci*., 1969, **116**, 832–835.
16. Lochner, R. H. and Matar, J. E., *Designing for Quality—An Introduction to the Best of Taguchi and Western Methods of Statistical Experimental Design*. Chapman and Hall, London, 1990.
17. Daniel, C., *Applications of Statistics to Industrial Experimentation*. John Wiley and Sons, New York, 1976.
18. Narendar, Y. and Messing, G. L., Mechanisms of phase separation in gel-based synthesis of multicomponent metal oxides. *Catal. Today*, 1997, **35**, 247–268.